

Proposed Guidelines for Selection of Methods for Erosion-corrosion Testing in Flowing Liquids

Masanobu Matsumura

237-101 Fukumoto, Saijo-cho, Higashi-Hiroshima 739-0031 JAPAN

The corrosion of metals and alloys in flowing liquids can be classified into uniform corrosion and localized corrosion which may be categorized as follows.

(1) Localized corrosion of the erosion-corrosion type: the protective oxide layer is assumed to be removed from the metal surface by shear stress or turbulence of the fluid flow. A macro-cell may be defined as a situation in which the bare surface is the macro-anode and the other surface covered with the oxide layer is the macro-cathode.

(2) Localized corrosion of the differential flow-velocity corrosion type: at a location of lower fluid velocity, a thin and coarse oxide layer with poor protective qualities may be produced because of an insufficient supply of oxygen. A macro-cell may be defined as a situation in which this surface is the macro-anode and the other surface covered with a dense and stable oxide layer is the macro-cathode.

(3) Localized corrosion of the active/passive-cell type: on a metal surface a macro-cell may be defined as a situation in which a part of it is in a passivation state and another in an active dissolution state. This situation may arise from differences in temperature as well as in the supply of the dissolved oxygen. Compared to uniform corrosion, localized corrosion tends to involve a higher wall thinning rate (corrosion rate) due to the macro-cell current as well as to the ratio of the surface area of the macro-anode to that of the macro-cathode, which may be rationalized using potential vs. current density diagrams. The three types of localized corrosion described above can be reproduced in a Jet-in-slit test by changing the flow direction of the test liquid and arranging environmental conditions in an appropriate manner.

Keywords : Jet-in-slit test, macro-cell corrosion, uniform corrosion, localized corrosion

1. Introduction

Erosion-corrosion is a major problem in industries handling liquids which may be flowing rapidly, are corrosive, and may be at high temperatures and high pressures. This mode of corrosion usually leads to rapid metal loss with possibly catastrophic consequences. In order to prevent, mitigate and/or control these problems, it is important to determine the resistance to corrosion of materials used in plant construction. This may be then achieved after understanding how a test methodology reproduces a specific mode of corrosion. The WG14 on tribo-corrosion committee (Convened by Dr. J. J. Kim, KRIS), TC156 for the Corrosion of Metals and Alloys, ISO (International Organization for Standardization), decided at the meeting held in May 2006 in Tokyo to submit a New Work Item Proposal, the title of which is given above. A member of the working group from Japan, Prof. M. Matsumura,

undertook the preparation of the first draft of the NWIP. It was recently completed and the contents are presented below.

2. Principle

The corrosion of metals and alloys in flowing liquids are classified into uniform corrosion and localized corrosion. Compared to uniform corrosion, localized corrosion tends to involve a higher wall thinning rate due to the macro-cell current as well as to the surface area ratio of macro-anode to macro-cathode, which is rationalized in the following sections using potential vs. current-density diagrams.¹⁾

2.1 Uniform corrosion

The potential vs. current-density diagram in Fig. 1 is for the uniform corrosion which consists of the following cathode and anode reactions.

[†] Corresponding author: mmatsu@rapid.ocn.ne.jp

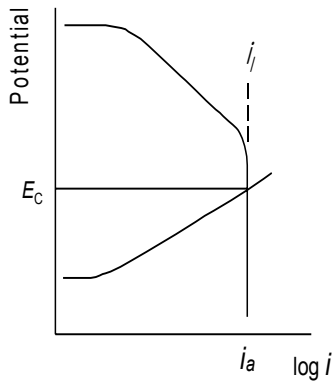
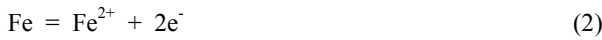


Fig. 1. Potential vs. current density diagram for uniform corrosion



At the point of intersection of the polarization curves, the criteria of conservation, that is, “anodic current = cathodic current” is satisfied. The coordinates at this point give the corrosion potential, E_c , and the corrosion current density, i_a , that is to say, the wall thinning rate, w . In the figure, the corrosion rate is equal to the oxygen diffusion limiting current-density, i_l , of cathodic polarization curve. This current-density is the largest transfer rate for oxygen as it migrates by diffusion from the bulk through the boundary layer to the metal surface, and it is not dependent on the potential. According to Eq. 1, the electric quantity of F (Faraday, 96500 Coulomb eq⁻¹) flows when 1/4 mol of oxygen reaches the metal surface and is consumed there. For the steady state,

$$i_a = i_l = (1/4)N_{O_2}F \quad (3)$$

where N_{O_2} is the migration rate of oxygen through the boundary layer, and is given by the product of the mass transfer coefficient, k , and the driving force for the migration which is the difference in oxygen concentration between the bulk and the metal surface, that is, C_b and C_o .

$$N_{O_2} = k (C_b - C_o) \quad (4)$$

Assuming that oxygen is consumed (reduced) as soon as it reaches the metal surface, C_o is 0, and N_{O_2} accordingly depends on the mass transfer coefficient and the dissolved oxygen concentration in the bulk of the liquid.

The mass transfer coefficient, k , is dependent on flow conditions and the physical properties of the liquid under consideration. In general, the relation is given using the dimensionless numbers as follows.

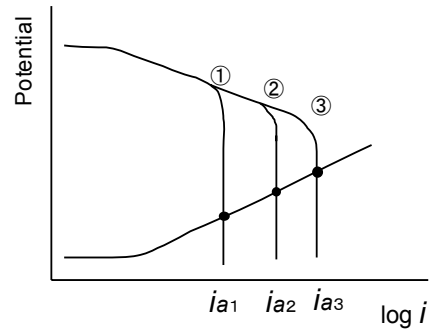


Fig. 2. Influence of flow velocity on the rate of uniform corrosion

$$Sh = c(Re)^a(Sc)^b \quad (5)$$

The index, a , takes values of 0.5~1 depending on the conditions of flow and others. The rate of uniform corrosion, therefore, increases in proportion to the power of a for flow velocity, when the dissolved oxygen concentration is fixed. This is shown on the potential vs. current-density diagram in Fig. 2. It rises with the ascending flow velocity, 1, 2, 3, but never exceeds the oxygen diffusion limiting current density.

2.2 Localized corrosion

2.2.1 Localized corrosion of erosion-corrosion type:

The most important feature of a potential vs. current-density diagram for localized corrosion is that it must contain at least two anodic polarization curves. The cathodic polarization curve may be one or two. For a comparison with those in Fig. 1 and 2, the two polarization curves are given respectively for the anodic and the cathodic reaction in the diagram of Fig. 3, where two zones with a common surface area, H and L , are assumed on a specimen of steel. It is also assumed that a liquid flow of higher velocity or a higher intensity of turbulence at zone H

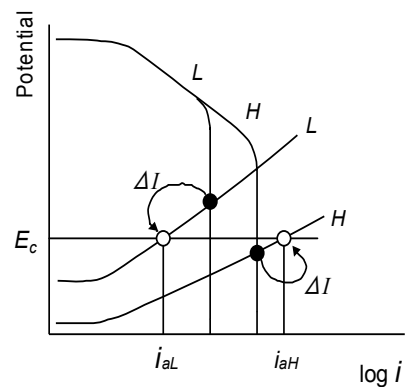


Fig. 3. Potential vs. current density diagram for localized corrosion of the erosion-corrosion type

would remove the protective oxide layer from the surface or at least clear the positive ions from the electrode surface resulting in a substantially lower polarization resistance for zone *H* as compared with that of zone *L*, which is shown in the diagram as the difference in the slopes of the anodic polarization curves. Concerning cathodic polarization, the assumption remains same as that of Fig. 2: the oxygen diffusion limiting current density at zone *H* is higher because of the higher oxygen supply rate due to the higher fluid velocity in that region. When these zones exist independently, the corrosion potentials are different from each other, as shown by the solid dots in the diagram at which the conservation, “anodic current = cathodic current”, is satisfied for each of them, the same as the case of uniform corrosion. The combination of zone *H* and *L* comprises a macro-cell where zone *H* becomes the macro-anode, and the metal is oxidized at a rate i_{aH} which is higher than when the zone corrodes independently. In contrast, zone *L* becomes the macro-cathode, and the metal is oxidized at a rate i_{aL} which is lower than when it corrodes independently. This is because the potentials move to an identical level as shown by the open dots where “the total anodic currents = the total cathodic current” is satisfied. Thus, in order for the criteria of conservation to be satisfied, the anodic current of zone *H* must be increased by an increment ΔI , and that of zone *L* must be decreased by the same amount, because the cathodic currents of both zones do not change before and after the formation of the macro-cell.

The increment ΔI is called the macro-cell current which causes the anodic current of zone *H* increase beyond the oxygen diffusion limiting current. This is the above mentioned “macro-cell current effect” and is one of the important mechanisms that brings higher wall thinning rates to localized corrosion.

Here, it should be also stated that the macro-cell current is not a current density but a current, that is, it does not have the dimension of $[A\ m^{-2}]$ but of $[A]$. A current divided by the surface area of zone is a current density or a wall thinning rate. Until now, a common surface area was assumed for zones *H* and *L*. Now the surface area of zone *H* is assumed to be smaller than that of zone *L* is, so that the current density as well as the wall thinning rate at zone *H* increases farther. This is the “area ratio effect,” which was referred to in the preceding section as another mechanism associated with increasing the rate of localized corrosion.

2.2.2 Localized corrosion of differential flow-velocity corrosion type:

The potential vs. current density diagram in Fig. 4 shows differential flow-velocity corrosion, where an alter-

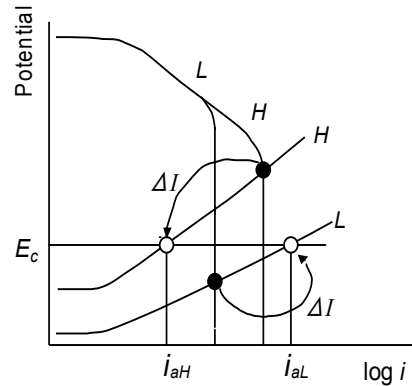


Fig. 4. Potential vs. current density diagram for localized corrosion of the differential flow-velocity corrosion type

native assumption is given: a larger anodic polarization resistance for zone *H*. This is because the elution of positive ions is suppressed by a dense and stable oxide film with excellent protective qualities over the surface, which is produced by a sufficient supply of oxygen as well as negative ions. Concerning cathodic polarization, the assumption remains the same as that of Fig. 3. In contrast to that in Fig. 3, the combination of zones comprises a macro-cell where zone *H* is the macro-cathode and zone *L* the macro-anode. In this case, zone *L*, which is exposed to a lower flow velocity, becomes a macro-anode and the metal is oxidized at a rate higher than that of the oxygen diffusion limiting current at zone *H*. The oxidation proceeds at a much higher rate when the “area ratio effect” is added.

2.2.3 Localized corrosion of the active/passive-cell type:

On the potential vs. current density diagram in Fig. 5, the reduction of hydrogen ions is taken up as the cathode reaction. That is to say, the environmental liquid is assumed in which the dissolved oxygen concentration is submerged so low that the reduction of oxygen no longer plays a major role in the cathode reaction. The hydrogen

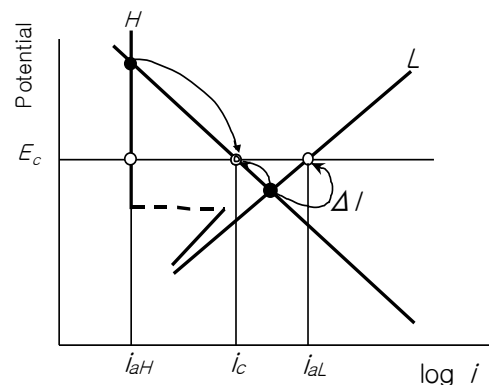


Fig. 5. Potential vs. current density diagram for localized corrosion of the active/passive-cell type

ion reduction reaction, the following Eq.6, proceeds alternatively and is independent of the oxygen diffusion limiting current as well as of flow velocity.



Suppose that the surface of zone *L* is covered with a fixed vortex or a stagnant lump of liquid which completely excludes the supply of oxygen to the surface. Traces of oxygen, however, might be supplied to the surface of zone *H* as it is exposed to a liquid flow of higher velocity compared with that at zone *L*. This situation might take the surface *L* into a state of activation and the surface *H* into passivation when the environmental temperature and pH are in the critical range which is characteristic to the metal. Once a macro-cell is formed in this couple, the anodic current density on the surface *H* does not change but that of surface *L* increases. This is because the potential of the macro-cell takes the level at which the balance in current, that is the following equation, is satisfied.

$$2I_c = I_{a1} + I_{a2} \quad (7)$$

Here again the macro-cell current flows from zone *H* to zone *L* increasing the anodic current density (macro-cell current effect). In the case where the surface of *L* is smaller than that of *H*, it increases still more (surface area ratio effect).

3. Testing methods

3.1 Methods for testing uniform corrosion

To reproduce uniform corrosion on a specimen, the flow of the test liquid must be uniform over the entire surface. This must be achieved regardless of how the relative speed between fluid and test specimen surface is caused: the rotating specimen method or the water tunnel method. The representative of the former is a submerged shaft shown in Fig. 6 which rotates in the liquid which is supposed



Fig. 6. A shaft rotating in the liquid at a standstill

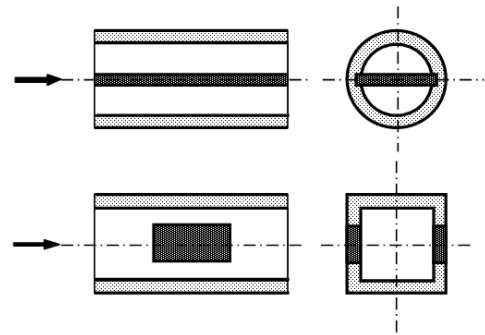


Fig. 7. Liquid flow in a pipe or channel with specimen surfaces parallel with the flow direction

to be standing still. The flat plate specimen installed in the pipe line and the test specimens embedded in the wall of the duct are examples of the latter (Fig. 7). In cases of testing methods other than those mentioned above and the evaluation of the effect of flow, detailed reports²⁾ should be consulted.

3.2 Methods for testing localized corrosion of erosion corrosion type

To reproduce localized corrosion of any type, the flow of the test liquid must be not uniform over the surface of specimen. Localized corrosion of the erosion-corrosion type may be reproduced on the specimens on a rotating disk and impinging jet systems³⁾. In the rotating disk method shown in Fig. 8, the flow over the test surface, that is the underside surface of disk, is rather complicated because the circumferential relative flow caused by the rotation overlaps with the radial secondary flow.

Among the impinging jet systems in Fig. 9, the Jet-in-slit has proved its usefulness, in the forms of reproducing localized corrosion of different types. The principle of a Jet-in-slit is illustrated in Fig. 10. Two circular disc surfaces with same diameter are oriented face to face with a narrow gap (slit) formed between the two surfaces. A hole is bored through the center of the upper disc, thus converting it to a nozzle with a large external diameter.

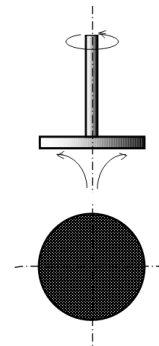


Fig. 8. A rotating disc

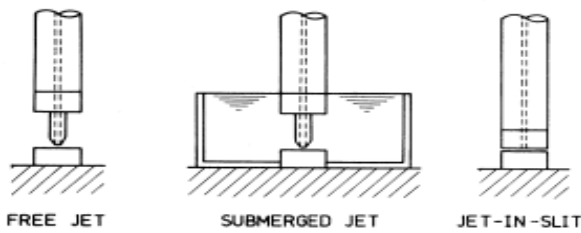


Fig. 9. Impinging jets used to evaluate localized corrosion

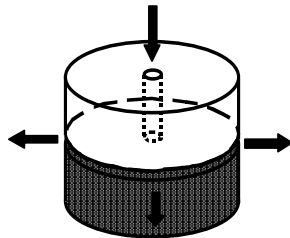


Fig. 10. The principle of the Jet-in-slit with ordinary flow; upper disc with a hole, the nozzle; lower disc, specimen

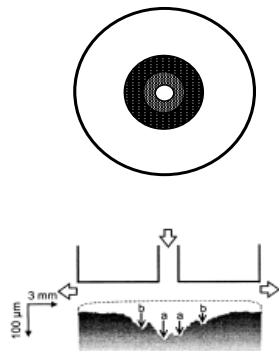


Fig. 11. Cross section of a pure copper specimen; a, damage due to shear stress; b, damage due to turbulence in the flow

A jet of the test liquid from the nozzle is allowed to impinge on the specimen (the lower disc), at right angles and then to flow in a radial direction through the gap. In this case, the arrangement is called ordinary flow. The dimensions of a typical arrangement are as follows: inside diameter of the nozzle, 1.6 mm; outside diameter of the nozzle and specimen, 16 mm; gap clearance, 0.8 mm.^{4,5)}

The advantage of a Jet-in-slit with ordinary flow is that the distribution of turbulence intensity as well as of shear stress over the specimen surface has already been determined. The shear stress reaches a maximum at the periphery of impinging liquid jet, whereas the turbulence intensity did so at the zone surrounding it. The cross section of a pure copper specimen after a 1 h test using a 1% $\text{CuCl}_2(\text{II})$ solution shown in Fig. 11 visualizes the situation: the ring shaped damage, *a*, is caused by shear stress and damage, *b*, by the turbulence in the fluid flow.⁶⁾

3.3 Methods for testing localized corrosion of differential flow-velocity corrosion type

A water tunnel with sudden convergence and divergence in the cross section of liquid flow as shown in Fig. 12, may reproduce differential flow-velocity corrosion on the inside surface of the tunnel wall which is essentially the test surface, as the stagnant lump of fluid or fixed vortices may be built at the downstream of the boundary layer separation points which are usually located at the corner tips where the cross section of flow changes suddenly.⁷⁾

The Jet-in-slit with a reverse flow shown in Fig. 13 has the same set up as that in Fig. 10, but the test liquid is fed from the outside of the gap to the center of the specimen and is then aspirated through the nozzle. No turbulence occurs in the flow at all, because the flow velocity increases monotonously as it flows from the circumference

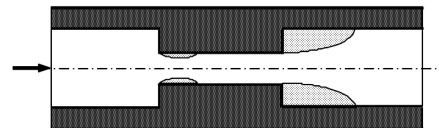


Fig. 12. Flow channel with sudden convergence and divergence

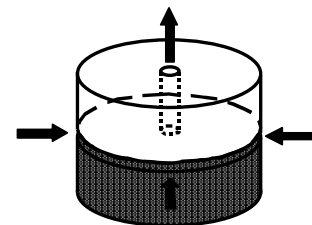


Fig. 13. The principle of Jet-in-slit with reverse flow; upper disc, nozzle; lower disc, specimen

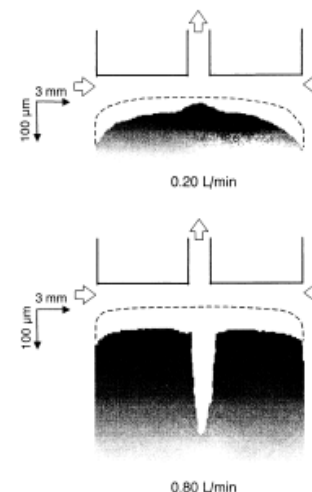


Fig. 14. Cross section of a pure copper specimen after a 1 h Jet-in-slit test with reverse flow of 1% $\text{CuCl}_2(\text{II})$ solution; upper, 0.20 L min^{-1} ; lower, 0.80 L min^{-1}

of the test specimen toward its center. According to the test results shown in Fig. 14, the shear stress is also seemingly lowered, to a negligible extent, because under conditions of a smaller flow rate, wall thinning grew at the peripheral zone where the flow velocity was lower than that at the central zone (Fig. 13, upper). In contrast, a deep penetration occurred just under the nozzle mouth when the flow rate was larger (Fig. 13, lower). This is because a fixed vortex was generated immediately under the exit nozzle. Thus, another type of the differential flow-velocity corrosion was reproduced.⁶⁾

3.4 Methods for testing localized corrosion of active/passive-cell type

The key point in methodology for reproducing localized corrosion of this type is to put part of the specimen surface into a passivation state and another part into an activation state. Fig. 15 shows an example of a set up for this purpose: two Jet-in-slit sets are coupled in series where the liquid is allowed to flow through the first in an ordinary

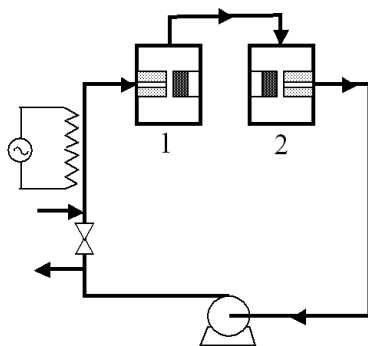


Fig. 15. Jet-in-slit apparatus used in a corrosion test under high pressure at elevated temperatures

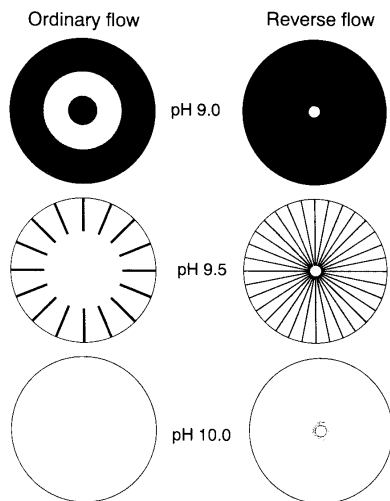


Fig. 16. Scheme showing corrosion morphology in various pH environments

way and the second in a reverse way. Tests can be carried out in environments in the critical temperature range where carbon steels may be in passivity or not, depending on other influencing factors.

Fig. 16 shows some results obtained using this set up. Test specimen surfaces of carbon steel were exposed to deoxidized pure water, the temperature of which was fixed at the critical range. As the pH of the liquid was increased, the state of the test surface changed from the full face active state (pH 9) to co-existing active state and passivity (pH 9.5), and then further to full face passivity (pH10). At pH 9.5, the narrow zone of the test specimen surface under string-shaped vortexes, which originated radial on the specimen surface, showed an active state, and the remainder passivity. The penetration rate at the narrow zone was as high as 1 mm y^{-1} , verifying that an active/passive-cell type corrosion was reproduced.⁸⁾

4. Conclusions

In selecting methods for erosion corrosion testing in flowing liquids, the following conditions are indispensable.

- 1) In selecting testing methods, it should be first determined which mode of erosion-corrosion is intended to be reproduced, and the method that can then reproduce it should be chosen.
- 2) The flow conditions over the specimen surface must be clearly verified, irrespective of the chosen testing method

References

1. M. Matsumura, *Materials and Corrosion*, **57**, 872 (2006).
2. G. Schmitt and M. Bakalli, Paper #06593, NACE Corrosion 2006, (2006)
3. M. Matsumura, Y. Oka, S. Okumoto and H. Furuya, "Laboratory Corrosion Tests and Standards", ASTM STP 866, p.358, American Society for Testing and Materials, Philadelphia, 1985.
4. M. Matsumura, Y. Oka and H. Yokohata, *Boshoku-Gijutsu* (presently *Zairyo-to-Kankyo*), **35**, 706 (1986).
5. M. Matsumura, *Proc. of Second International Conference on Environment Sensitive Cracking and Corrosion Damage*, p.3, (2001).
6. M. Murakami, A. Yabuki and M. Matsumura, *Zairyo-to-Kankyo*, **52**, 160 (2003).
7. T. Sydberger and V. Lotz, *J. Electrochem. Soc.*, **129**, 276 (1982).
8. S. Ohguni, A. Yabuki, M. Matsumura and K. Marugame, *Zairyo-to-Kankyo*, **50**, 386 (2001).